ELECTRONIC SUPPLEMENTARY INFORMATION (ESI) FOR:

Trapping an unprecedented octacoordinated iron(II) complex with neutral *bis*-tetrazolylpyridyl ligands and solvent molecules

Luca Rigamonti, Lorenzo Marchi, Valentina Fiorini, Stefano Stagni, Stefano Zacchini, Dawid Pinkowicz, Katarzyna Dziedzic-Kocurek, Alessandra Forni, Francesco Muniz Miranda and Rita Mazzoni

Index

Experimental Section

General information. All chemicals were reagent grade and solvents were used as received. Petroleum ether (PE) was the fraction with boiling range 40-60 °C. Elemental analyses were performed with the Thermo Scientific Flash 2000 (CHNS analyser) instrument. ^{1}H and ^{13}C NMR spectra were recorded at 298 K on Varian Mercury Plus VX400 (^{1}H, 399.9; ^{13}C, 100.6 MHz) spectrometer. Proton and carbon chemical shifts are given in parts per million (ppm) versus external TMS, and they were determined by reference to the solvent residual signals (^{1}H NMR: 7.26 ppm, ^{13}C NMR: 77.0 ppm for CHCl$_3$); coupling constants are given in Hz. Infrared spectra were recorded as ATR spectra using a Jasco FTIR-4700LE or a Perkin Elmer FTIR-IRL1600300 spectrophotometer equipped with a diamond tip for solids and with a 2 cm^{-1} resolution; bands are reported as wavenumbers (cm^{-1}) together with their assignments and relative intensity (vs = very strong, s = strong, m = medium, w = weak, br = broad). 2,6-di(2*H*-tetrazol-5-yl)pyridine (H$_2$btp) was synthesized as previously reported.[1,2]

Synthesis of 2,6-*bis*(2-(methyl)-2*H*-tetrazol-5-yl)pyridine (Me$_2$btp). This ligand was prepared by adapting a procedure reported in the literature.[3] H$_2$btp (0.500 g, 2.32 mmol) was dissolved in MeCN (25 mL) in the presence of an excess of K$_2$CO$_3$. The mixture was refluxed for 1 h and then MeI was added (0.36 mL, 5.8 mmol). The resulting reaction mixture was refluxed for further 18 h, then cooled to room temperature and the solvent was removed by rotary evaporation. The obtained crude mixture was treated with CH$_2$Cl$_2$ causing the precipitation of K$_2$CO$_3$, which was filtered off through a glass frit, followed by washing with CH$_2$Cl$_2$ (3 × 10 mL). The so-obtained organic phase was purified by column chromatography on silica using Et$_2$O:PE 1:1 (*v/v*) as eluent. The desired *N2-N2* isomer was eluted as third fraction and recovered as white amorphous powder after removal of the solvent. Yield: 0.230 g, 41%. Anal. (%) Calcd. for C$_9$H$_9$N$_9$ (243.23): C 44.44, H 3.73, N 51.83. Found: C 44.65, H 3.71, N 51.60. ^{1}H NMR (399.9 MHz, 298 K, CDCl$_3$): δ 8.34 (d, $J_{H,H}$ = 8.0 Hz, 2H, H$_{py,meta}$), 8.05 (t, $J_{H,H}$ = 8.0 Hz, 1H, H$_{py,para}$), 4.50 (s, 6H, CH_3) ppm. ^{13}C NMR (100.6 MHz, 298 K, CDCl$_3$) δ 164.34 (C$_{tetrazole}$), 147.38 (C$_{py,ortho}$), 138.37 (C$_{py,para}$), 123.39 (C$_{py,meta}$), 39.75 (CH_3) ppm. FT-IR (ATR, cm^{-1}): 3089w + 3038w + 2959w (νC–H), 1597m + 1579m (νC=N), 1422s + 1359m (δC–H,Me).

Synthesis of [Fe(Me$_2$btp)$_2$](ClO$_4$)$_2$·MeCN·2.75H$_2$O (2·MeCN·2.75H$_2$O). Solid Fe(ClO$_4$)$_2$·6H$_2$O (8.7 mg, 0.0239 mmol) was added to a colourless solution of Me$_2$btp (11.6 mg, 0.0479 mmol) in CH$_2$Cl$_2$ (1 mL) and MeCN (1 mL) yielding a yellow-orange solution. The reaction mixture was stirred for 30 mins and then filtered to eliminate some solid residue. The clear orange solution was stratified with Et$_2$O (4 mL) and after one week at complete diffusion, the solution became colourless with several well-formed

red rod-like crystals of **2**·MeCN·2.75H$_2$O, kept in their mother liquor and isolated each time by hand for all the analyses. Given by the colourless mother liquor, the yield could be considered practically quantitative. Anal (%) calcd for C$_{18}$H$_{18}$Cl$_2$FeN$_{18}$O$_8$·MeCN·2.75H$_2$O (831.80): C, 27.44; H, 3.21; N, 30.31. Found: C, 27.44; H, 2.92; N, 30.27. FT-IR (ATR, cm^{-1}): 3317m + 3220m (νO–H water), 2316w + 2291w + 2255w (νC≡N acetonitrile), 1616m (νC=N), 1424s + 1362m (δC–H methyl), 1076vs + 929w (νClO$_4$).

Characterization of [Fe(Me$_2$btp)$_2$(MeCN)(H$_2$O)](ClO$_4$)$_2$·H$_2$O (1·H$_2$O). Yellow crystals of the title compound were manually selected from a synthetic batch as reported above in MeCN:CH$_2$Cl$_2$ 1:3 mixture. Anal (%) calcd for C$_{20}$H$_{23}$Cl$_2$FeN$_{19}$O$_9$·H$_2$O (818.29): C, 29.36; H, 3.08; N, 32.52. Found: C, 29.45; H, 2.96; N, 32.28. FT-IR (ATR, cm^{-1}): 3566m + 3243w (νO–H water), 2313w + 2286w (νC≡N acetonitrile), 1616m (νC=N), 1448s + 1366m (δC–H methyl), 1074vs (νClO$_4$).

Characterization of [Fe(Me$_2$btp)$_2$][Fe(Me$_2$btp)(MeCN)$_2$(H$_2$O)](ClO$_4$)$_4$·MeCN (2·3·MeCN). Red crystals of the title compound were manually selected from a synthetic batch as reported above in MeCN:CH$_2$Cl$_2$ 1:1 mixture and after standing in solution for 3 months. Anal (%) calcd for C$_{31}$H$_{35}$Cl$_4$Fe$_2$N$_{29}$O$_{17}$·MeCN (1380.35): C, 28.71; H, 2.77; N, 30.44. Found: C, 28.92; H, 2.86; N, 30.21. FT-IR (ATR, cm^{-1}): 3566m + 3243w (νO–H water), 2314w + 2288w (νC≡N acetonitrile), 1616m (νC=N), 1438s + 1365m (δC–H methyl), 1078vs (νClO$_4$).

X-ray Crystal Structure Determinations. Crystal data and collection details for **1**·H$_2$O are reported in Table S1. The diffraction experiments were carried out on a Bruker APEX II diffractometer equipped with a PHOTON100 detector and using Mo-Kα radiation at 100(2) K. Data were corrected for Lorentz polarization and absorption effects (empirical absorption correction SADABS).[4] Structure was solved by direct methods and refined by full-matrix least-squares based on all data using F^2.[5] All non-hydrogen atoms were refined with anisotropic displacement parameters.

Only one half of the [Fe(Me$_2$btp)$_2$(MeCN)(H$_2$O)]$^{2+}$, located on a 2-*axis*, was present in the asymmetric unit of the unit cell. The MeCN and H$_2$O ligands were disordered over two equally populated symmetry-related (by 2) positions. The N and O atoms of the MeCN and H$_2$O ligands were constrained to have identical thermal parameters (EADP line in SHELXL). The H atoms bonded to C-atoms were fixed at calculated positions and refined isotropically using a riding model. The H atoms bonded to the Fe-coordinated H$_2$O molecule were preliminarily located in the Fourier Difference Map and, then refined using a riding model (AFIX 93 line in SHELXL; this sets the O10-H10a and O10-H10b

distances to 0.95 Å). The H atoms of the free H_2O molecule were located on the Fourier Difference Map and refined isotropically using the 1.5-fold U_{iso} of the parent O-atom and restraining the O–H distances (DFIX 0.91 0.001 O11 H111 O11 H112 line in SHELXL). All X-H distances (including those of the Fe-coordinated H_2O molecule) have been set using the default values of SHELXL, except those of the free H_2O molecule which have been restrained to 0.91 Å. The disorder is probably more complicated than that described by this model. In particular, it is very difficult to properly locate the H-atoms bonded to the water molecule coordinated to Fe. Thus, these H-atoms have been placed by a geometrical model. Moreover, the free water molecule is disordered over more positions than those described by our model. Because of this, some residual electron density is present (see picture below). Nonetheless, the coordination sphere of iron(II) and ligands could be properly located and modelled.
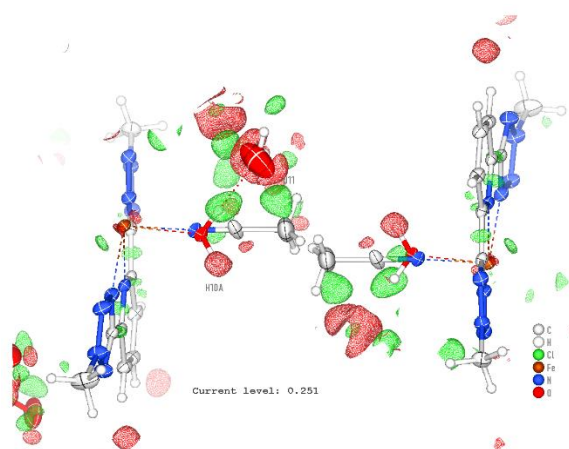
Crystal data and collection details of **2·3·MeCN** are reported in Table S5. The diffraction experiments were carried out using Bruker D8QuestEco three-circle diffractometer equipped with a PhotonII detector, Mo-Kα ($\lambda = 0.71073$ Å) sealed tube X-ray source, multilayer Triumph monochromator and Oxford Cryostream 700+ low temperature device. The selected crystals were mounted on cryoloops using PEG cryoprotectant. Lorentz polarization and multi-scan absorption corrections were applied using SADABS. The crystal structures were solved by intrinsic phasing with the use of the Apex3 suite of programs, and the structural models were refined by full-matrix least squares technique on F^2 using SHELXL.

The program Mercury 4.3.1 was used for graphics.[6]

CCDC 2299246, 2295757 and 2295758 contain the supplementary crystallographic data for **1·H_2O** at 100 K, **2·3·MeCN** at 100 K and **2·3·MeCN** at 270 K, respectively. These data can be obtained free of charge via https://www.ccdc.cam.ac.uk/structures/, or from the Cambridge Crystallographic Data Centre, 12 Union Road, Cambridge CB2 1EZ, UK; fax: (+44) 1223-336-033, or e-mail: deposit@ccdc.cam.ac.uk.

Powder X-ray diffraction. PXRD data were recorded using Bruker D8AdvanceEco diffractometer with Cu-Kα radiation (λ = 1.5406 Å) at room temperature for ground crystalline samples loaded into glass capillaries.

Mössbauer spectroscopy. The transmission ^{57}Fe Mössbauer spectra were recorded using a WisseEl spectrometer (Wissenschaftliche Electronic GmbH, Ortenberg, Germany) equipped with a liquid nitrogen cryostat. The spectra were collected in 1024 channels, with a ~5 mCi ^{57}Co source in an Rh matrix. The sample sealed inside a polyethylene (PE) bag was enclosed within two pieces of mylar foil in a 12 mm diameter cooper ring. The temperature stability was 0.1 K and the temperature distribution over the sample less than 1 K. The velocity scale was calibrated using the α-Fe foil standard. The reported spectra were numerically evaluated with the *WinNormos-for-Igor package* (Wissenschaftliche Electronic GmbH, Ortenberg, Germany), assuming the Lorentzian shape of the resonance lines, i.e., the saturation effects were not included, and considering the temperature effect of the Debye-Waller factor.

Magnetic measurements. Magnetic measurements on a polycrystalline red sample of **2**$^{\text{HS/LS}}$·MeCN·2.75H$_2$O kept in its mother liquor and vacuum sealed in a borosilicate tube were performed using a Quantum Design MPMS3 magnetometer equipped with a 7 T magnet. The magnetic measurements were then repeated once the crystals were allowed to convert into yellow of **2**$^{\text{HS}}$·solvent. The temperature dependence of χ_M (molar magnetic susceptibility) was recorded from 1.8 to 250 K under the applied magnetic field H_{DC} = 1 kOe, while he $M_M(H)$ curve (M_M = molar magnetization) were recorded at 1.8 K in the range of 0–7 T. The magnetic data were corrected for the sample holder contributions and for the sample diamagnetism calculated from Pascal's constants.[7]

Computational Details. Geometry optimization of **1**, **2** and **3** dications in the HS state were performed. Geometry relaxations, counterpoise calculations (to obtain binding energies, BEs), and energy scans were performed at the quantum-chemistry DFT level employing the Gaussian 16 suite of software.[8] The all-electron 6-311G(d) basis set has been adopted, in conjunction with the M06 exchange-correlation functional: the latter choice of functional is due to M06 having been devised specifically to better reproduce the thermodynamics of compounds containing transition metals.[9] Each relaxed structure has real and positive vibrational frequencies.

The BEs were calculated for the **2**$^{\text{HS}}$, **1**$^{\text{HS}}$, **3**$^{\text{HS}}$, and **2**$^{\text{LS}}$:

BE(**2**$^{\text{HS}}$) = 2 × BE(Me$_2$btp) = 2 × −134 (±5) = −268 (±10) kcal/mol

BE($\mathbf{1}^{HS}$) = 2 × BE(Me$_2$btp) + BE(MeCN) + BE(H$_2$O) = 2 × –97 (±6) –27 (±2) –20 (±2) = –241 (±10) kcal/mol

BE($\mathbf{3}^{HS}$) = 2 × BE(MeCN) + BE(H$_2$O) + BE(Me$_2$btp) = 2 × –36 (±4) –23 (±5) –145 (±4) = –240 (±13) kcal/mol

BE($\mathbf{2}^{LS}$) = 2 × BE(Me$_2$btp) = 2 × –170 (±7) = –340 (±14) kcal/mol

In these calculations, the quantity BE(molecule) can assume different values depending on the rest of the complex to which it is linked: as an example, BE(H$_2$O) is 20 kcal/mol in $\mathbf{1}^{HS}$, while it is 23 kcal/mol in $\mathbf{3}^{HS}$. The reported uncertainties correspond to the basis set superposition error (BSSE) correction.

Relaxed energy scans to explore the mechanism of conversion from $\mathbf{2}^{HS}$ to $\mathbf{1}^{HS}$ were performed according to the following procedure. First, the reverse $\mathbf{1}^{HS} \rightarrow \mathbf{2}^{HS}$ path was simulated to make calculation feasible. Starting from the optimized geometry of $\mathbf{1}^{HS}$, the two solvent molecules were gradually displaced, at first separately, from the iron(II) centre. In other words, two energy scans were computed, one for the [Fe(Me$_2$btp)$_2$(MeCN)(H$_2$O)]$^{2+}$ $\rightarrow$ [Fe(Me$_2$btp)$_2$(MeCN)]$^{2+}$ + H$_2$O process and the other for the [Fe(Me$_2$btp)$_2$(MeCN)(H$_2$O)]$^{2+}$ $\rightarrow$ [Fe(Me$_2$btp)$_2$(H$_2$O)]$^{2+}$ + MeCN process. The scans were performed by increasing, respectively, the H$_2$O⋯Fe or MeCN⋯Fe distances with 0.1 Å step and optimizing the geometry of the whole system. During the MeCN removal scan, we noticed the gradual establishment of O–H⋯N hydrogen bond (HB) between the coordinated water molecule and the departing acetonitrile. Based on this HB configuration, we therefore proceeded with a single relaxed scan by gradually increasing the H$_2$O⋯Fe distance, with MeCN now directly interacting with water, and therefore moving away with it. We stopped the scan when the water molecule was sufficiently far (> 6.5 Å) from the iron ion, that is, at a distance sufficiently long to allow a definite location of a saddle point. At the final geometry, the two solvent molecules can be certainly considered outside the iron coordination sphere, though they are still interacting with the external portions of the complex.

Table S1 Crystallographic and refinement data for **1**·H_2O at 100 K.

	1·H_2O
Formula	$C_{20}H_{25}Cl_2FeN_{19}O_{10}$
M	818.34
Temperature / K	100(2)
radiation λ / Å	Mo-Kα, 0.71073
Crystal system	monoclinic
Space group	$C2/c$ (n. 15)
a / Å	21.6089(6)
b / Å	10.0066(3)
c / Å	15.0212(4)
β / °	96.4620(10)
V/Å^3	3227.42(16)
Z	4
D_c/ g cm^{-3}	1.684
μ / mm^{-1}	0.717
F(000)	1672
Colour, habit	yellow, prism
Crystal size / mm	$0.19 \times 0.15 \times 0.12$
θ limits / °	1.897–25.999
Measured reflns	21820
Independent reflns	3181
Reflns with $I>2\sigma(I)$	3053
R_{int}	0.0262
R_1, wR_2 [$I>2\sigma(I)$]	0.0432, 0.1078
R_1, wR_2 [all data]	0.0445, 0.1088
Goodness of fit on F^2	1.079
Parameters, restraints	261, 17
$(\Delta/\sigma)_{max}$	0.002
$\Delta\rho_{max}$, $\Delta\rho_{min}$ / e Å^{-3}	0.795, –0.580

Table S2 Experimental coordination bond distances (Å) and angles (°) of **1**·H_2O from X-ray diffraction, together with UM06/6-311+G(d) computed structural parameters for the dicationic species.

parameter [1]	X-ray value	Optimized geometry [2]
Fe1–N1	2.4413(19)	2.419, 2.525
Fe1–N5 (py)	2.3986(19)	2.407, 2.421
Fe1–N6	2.258(2)	2.266, 2.276
Fe1–N10 (CH_3CN)	2.12(2)	2.213
Fe1–O10 (H_2O)	2.286(19)	2.255
N1–Fe1–N5	66.53(6)	66.57, 65.85
N5–Fe1–N6	69.01(7)	69.30, 69.11
N1–Fe1–N6	135.09(7)	135.87, 134.91
N10–Fe1–N1	75.1(5)	78.54, 73.01
O10–Fe1–N1	80.4(4)	73.20, 75.82
N10–Fe1–N5	77.9(6)	78.84
O10–Fe1–N5	79.0(4)	77.21
N10–Fe1–N6	101.7(6)	93.62
O10–Fe1–N6	97.3(5)	92.43
N1–Fe1–N1#1	140.21(10)	136.19
N1–Fe1–N5#1	131.29(6)	133.30, 135.90
N1–Fe1–N6#1	77.26(7)	79.23, 76.85
N5–Fe1–N5#1	131.30(6)	132.76
N5–Fe1–N6#1	78.88(7)	79.14, 79.20
N10–Fe1–N1#1	75.7(6)	73.01, 78.54
O10–Fe1–N1#1	71.4(4)	75.82, 73.20
N10–Fe1–N5#1	141.2(6)	138.86
O10–Fe1–N5#1	137.6(4)	139.77
N10–Fe1–N6#1	149.2(6)	151.96
O10–Fe1–N6#1	153.3(4)	150.93

[1] symmetry code #1 = –x+1, y, –z+1/2 (referred only to the X-ray structure)
[2] the two values of distances and angles correspond to the two Me_2btp ligands

Table S3 Summary of Continuous Shape Measurement (CShM) calculations[10] on the coordination polyhedron of the iron(II) centre in **1**·H_2O.

		symmetry	deviation
OP-8	Octagon	D_{8h}	31.427
HPY-8	Heptagonal pyramid	C_{7v}	25.204
HBPY-8	Hexagonal bipyramid	D_{6h}	14.914
CU-8	Cube	O_h	11.872
SAPR-8	**Square antiprism**	**D_{4d}**	**2.776**
TDD-8	**Triangular dodecahedron**	**D_{2d}**	**1.084**

Table S4 Hydrogen bonds (Å and °) for **1**·H_2O.

D–H···A	d(D–H)	d(H···A)	d(D···A)
C5–H5···O10#2	0.95	2.65	3.531(17)
C8–H8A···O3#3	0.98	2.41	3.197(4)
C8–H8B···O2#4	0.98	2.39	3.355(4)
C8–H8C···O3#5	0.98	2.63	3.331(4)
C9–H9A···N4#6	0.98	2.54	3.269(4)
C9–H9B···O4#7	0.98	2.46	3.445(4)
C12–H12B···N9#3	0.98	2.61	3.322(7)
O10–H10A···N9#2	0.95	2.58	3.278(16)
O10–H10B···O4#3	0.95	2.52	3.128(18)
O11–H111···O1#8	0.92(2)	2.14(2)	2.943(9)
O11–H112···O1#3	0.979(16)	2.198(15)	3.175(8)
C5–H5···O10#2	0.95	2.65	3.531(17)
C8–H8A···O3#3	0.98	2.41	3.197(4)
C8–H8B···O2#4	0.98	2.39	3.355(4)

Symmetry transformations used to generate equivalent atoms:
#2 = –x+1, –y+1, –z+1; #3 = x, y+1, z; #4 = x, –y+1, z–1/2;
#5 = –x+3/2, y+1/2, –z+1/2; #6 = x–1/2, y–1/2, z;
#7 = –x+1, –y, –z+1; #8 = –x+1, y+1, –z+1/2
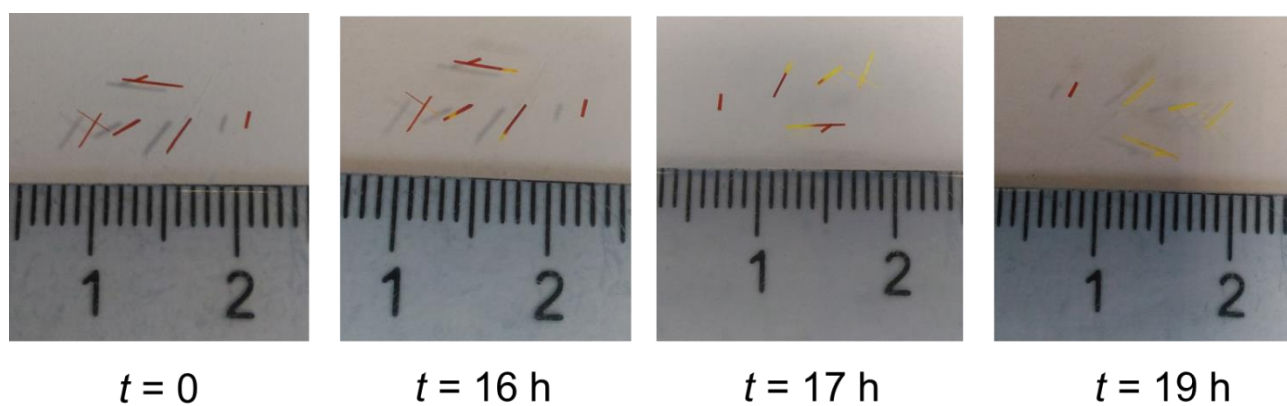
Fig. S1 Transformation of $2^{HS/LS} \cdot MeCN \cdot 2.75H_2O$ from red to yellow rods at ambient conditions.
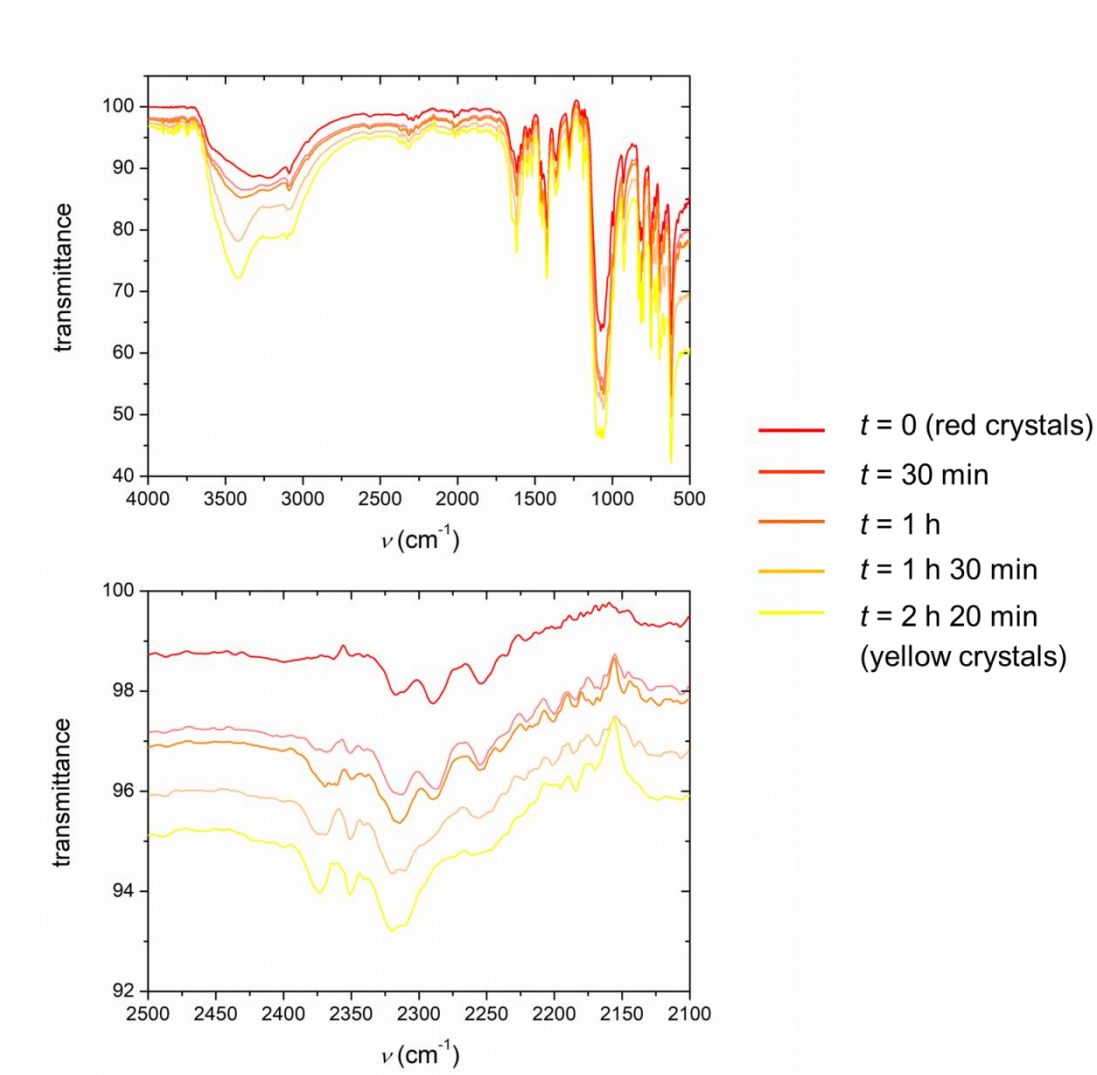
Fig. S2 FT-IR study in ATR mode of the conversion of $2^{HS/LS} \cdot MeCN \cdot 2.75H_2O$ from red to yellow crystals.
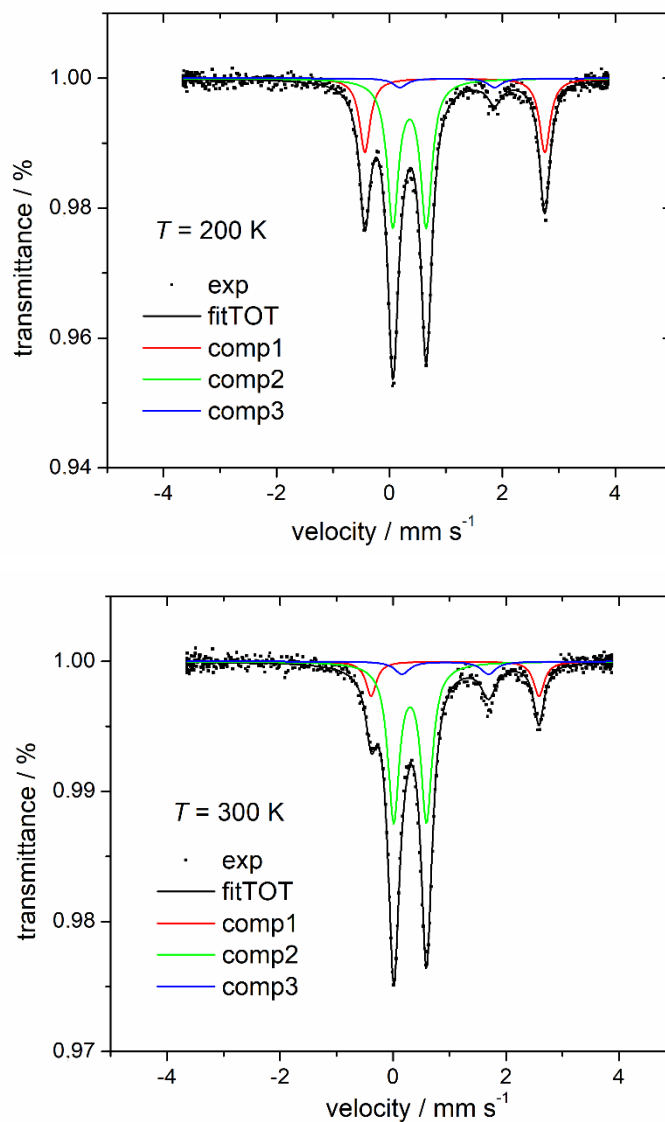
Fig. S3 Mossbauer spectra of **2**[HS/LS]·MeCN·2.75H$_2$O at 200 and 300 K, together with the fitting of the experimental data (black line) due to the presence of three different components (comp1 = HS iron(II) centres, comp2 = LS iron(II) centres, comp3 = **1**·H$_2$O present as < 5% impurity).

Table S5 Fitting parameters of the experimental Mossbauer spectra of $\mathbf{2}^{HS/LS}\cdot MeCN\cdot2.75H_2O$ shown in Figs. 3 and S3 at three different temperatures (100, 200 and 300 K) by assuming three different species: HS iron(II) centres as component 1 (red line), LS iron(II) centres as component 2 (green line) and $\mathbf{1}\cdot H_2O$ as component 3 (blue line). Noteworthy, the spectrum taken at 300 K shows a change in the ratios between the different species, proving that above 250 K the sample tends to interconvert.

T / K	Line width / mm·s⁻¹			Isomeric shift / mm·s⁻¹			Quadruple splitting / mm·s⁻¹			Integral		
	Comp.1	Comp.2	Comp.3	Comp.1	Comp.2	Comp.3	Comp.1	Comp.2	Comp.3	Comp.1	Comp.2	Comp.3
100	0.226(3)	0.230(2)	0.36(3)	1.207(1)	0.389(1)	1.14(1)	3.360(2)	0.598(1)	1.67(2)	0.46(2)	0.48(2)	0.06(2)
200	0.230(4)	0.240(2)	0.30(4)	1.157(1)	0.356(1)	1.03(1)	3.187(3)	0.592(1)	1.68(2)	0.50(2)	0.47(2)	0.03(2)
300	0.23(1)	0.242(2)	0.32(3)	1.097(3)	0.302(1)	0.925(8)	2.973(7)	0.584(2)	1.53(2)	0.37(2)	0.57(2)	0.06(2)

Table S6 Crystallographic and refinement data for $\mathbf{2}^{LS}\cdot\mathbf{3}^{HS}\cdot$MeCN at 100 and 270 K.

	100 K	270 K
Formula	$C_{33}H_{38}Cl_4Fe_2N_{30}O_{17}$	$C_{33}H_{38}Cl_4Fe_2N_{30}O_{17}$
M	1380.43	1380.43
Temperature / K	100(2)	270(2)
radiation λ / Å	Mo-Kα, 0.71073	Mo-Kα, 0.71073
Crystal system	monoclinic	monoclinic
Space group	$P2_1/n$ (n. 14)	$P2_1/n$ (n. 14)
a / Å	12.9623(6)	13.2592(3)
b / Å	13.6092(6)	13.7152(3)
c / Å	31.4613(13)	31.6336(7)
β / °	99.282(2)	99.4640(10)
V / Å^3	5477.3(4)	5674.4(2)
Z	4	4
D_c / g cm^{-3}	1.674	1.614
μ / mm^{-1}	0.821	0.792
F(000)	2808	2808
Colour, habit	red, prism	red, prism
Crystal size / mm	$0.16 \times 0.14 \times 0.07$	$0.16 \times 0.14 \times 0.07$
θ limits / °	2.32–26.50	2.17–25.03
Measured reflns	72681	75116
Independent reflns	11340	10023
Reflns with $I>2\sigma(I)$	10108	8570
R_{int}	0.0481	0.0700
R_1, wR_2 [$I>2\sigma(I)$]	0.0633, 0.1222	0.0871, 0.1652
R_1, wR_2 [all data]	0.0721, 0.1253	0.1041, 0.1723
Goodness of fit on F^2	1.230	1.221
Parameters, restraints	884, 217	884, 169
$(\Delta/\sigma)_{max}$	0.001	0.001
$\Delta\rho_{max}$, $\Delta\rho_{min}$ / e Å^{-3}	0.824, –0.527	0.669, –0.454

Table S7 Experimental coordination bond distances (Å) and angles (°) of 2^{LS}·3^{HS}·MeCN (Fe1 refers to 2^{LS} while Fe2 refers to 3^{HS}) from X-ray diffraction, together with UM06/6-311+G(d) computed structural parameters for the dicationic species of 2^{LS}, 2^{HS} and 3^{HS}.

parameter	100 K	270 K	2^{LS}	2^{HS}	3^{HS}
Fe1–N1A	1.946(3)	1.950(4)	1.986	2.223	-
Fe1–N5A (py)	1.924(3)	1.926(4)	1.957	2.168	-
Fe1–N6A	1.956(3)	1.960(4)	1.986	2.192	-
Fe1–N1B	1.949(3)	1.954(4)	1.984	2.223	-
Fe1–N5B (py)	1.925(3)	1.929(4)	1.957	2.168	-
Fe1–N6B	1.947(3)	1.953(4)	1.986	2.192	-
Fe2–N1C	2.221(3)	2.248(5)	-	-	2.232
Fe2–N5C (py)	2.184(3)	2.196(5)	-	-	2.191
Fe2–N6C	2.215(3)	2.223(5)	-	-	2.232
Fe2–N10C (MeCN)	2.149(3)	2.141(6)	-	-	2.146
Fe2–N11C (MeCN)	2.107(3)	2.116(6)	-	-	2.106
Fe2–O1 (H_2O)	2.070(3)	2.071(4)	-	-	2.185
N1A–Fe1–N5A	80.22(12)	80.05(18)	79.76	73.73	-
N5A–Fe1–N6A	80.55(12)	80.23(18)	79.76	74.58	-
N1A–Fe1–N6A	160.76(12)	160.27(11)	159.52	148.24	-
N1B–Fe1–N5B	80.29(12)	80.20(18)	79.83	73.72	-
N5B–Fe1–N6B	80.51(12)	80.22(18)	79.73	74.58	-
N1B–Fe1–N6B	160.80(12)	160.42(18)	159.57	148.23	-
N1A–Fe1–N1B	92.09(12)	91.97(18)	91.69	87.83	-
N1A–Fe1–N5B	96.91(12)	98.61(17)	100.24	94.74	-
N1A–Fe1–N6B	90.06(12)	90.54(17)	91.92	96.91	-
N5A–Fe1–N1B	100.33(12)	100.58(18)	99.99	94.73	-
N5A–Fe1–N5B	177.07(12)	178.45(19)	179.83	164.22	-
N5A–Fe1–N6B	98.84(12)	98.98(18)	100.42	116.80	-
N6A–Fe1–N1B	91.04(12)	91.10(18)	91.69	96.90	-
N6A–Fe1–N5B	102.33(12)	101.12(18)	100.24	116.78	-
N6A–Fe1–N6B	93.18(12)	93.06(18)	91.92	95.32	-
N1C–Fe2–N5C	73.75(11)	73.62(18)	-	-	73.62
N5C–Fe2–N6C	73.67(11)	73.60(17)	-	-	73.62
N1C–Fe2–N6C	147.40(11)	147.21(18)	-	-	146.48
N10C–Fe2–N11C	86.14(11)	86.4(2)	-	-	90.07
N10C–Fe2–O1	175.39(13)	172.9(2)	-	-	179.95
N11C–Fe2–O1	90.20(12)	90.3(2)	-	-	89.98

N1C–Fe2–N10C	86.36(12)	86.5(2)	-	-	93.87
N1C–Fe2–N11C	112.34(12)	113.5(2)	-	-	106.30
N1C–Fe2–O1	92.43(11)	89.04(18)	-	-	86.11
N5C–Fe2–N10C	89.21(12)	90.1(2)	-	-	91.50
N5C–Fe2–N11C	172.03(12)	171.9(2)	-	-	178.43
N5C–Fe2–O1	94.73(11)	93.91(19)	-	-	88.45
N6C–Fe2–N10C	94.12(12)	94.4(2)	-	-	93.89
N6C–Fe2–N11C	100.19(12)	99.28(19)	-	-	106.24
N6C–Fe2–O1	89.29(11)	92.29(19)	-	-	86.10
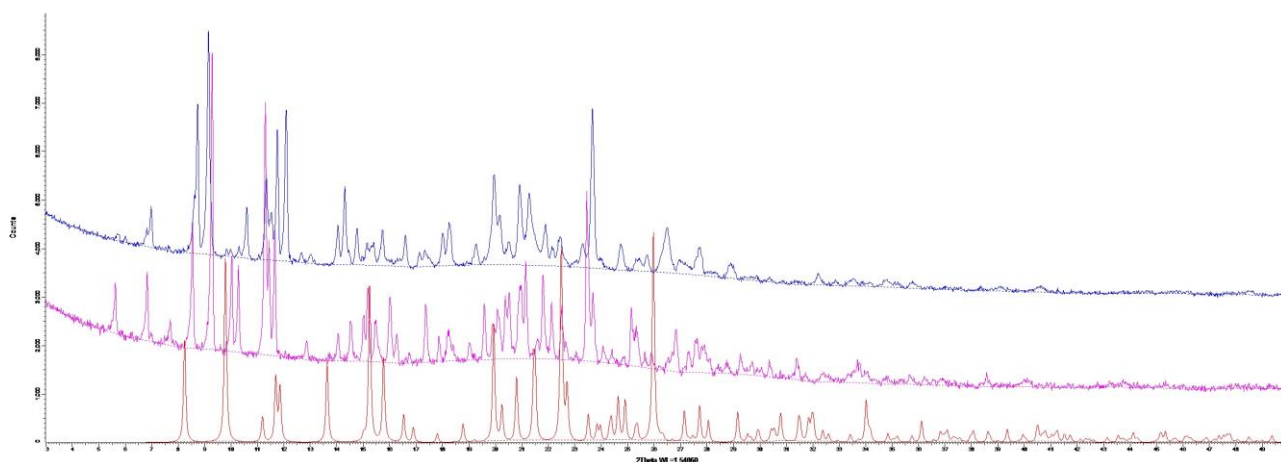
Fig. S4 Powder X-ray diffraction patterns of $2^{LS/HS}\cdot MeCN\cdot 2.75H_2O$ (magenta) and $2^{LS}\cdot 3^{HS}\cdot MeCN$ (blue), together with the simulated pattern from single crystal data of $1\cdot H_2O$ (red).

Table S8 UM06/6-311+G(d) coordination bond distances (Å) of 2^{HS}, 1^{HS} and the complexes appearing in the relaxed energy scan of the $2^{HS} \rightarrow 1^{HS}$ conversion mechanism (Fig. 4 of the main text).

parameter	2^{HS}	$2^{HS}+H_2O+MeCN$ (starting point)[1]	$2^{HS}\cdots H_2O\cdots MeCN$ (transition state)[1]	$2^{HS}\cdots H_2O\cdots MeCN$ (MeCN hydrogen bonded to H_2O)[1]	$1^{HS, 1}$
Fe1–N1	2.192	2.197, 2.188	2.192, 2.216	2.211, 2.266	2.419, 2.525
Fe1–N5 (py)	2.168	2.168, 2.166	2.179, 2.161	2.173, 2.222	2.407, 2.421
Fe1–N6	2.224	2.201, 2.205	2.206, 2.224	2.215, 2.186	2.266, 2.276
Fe1–N10 (MeCN)	-	4.398	5.373	4.503	2.213
Fe1–O10 (H_2O)	-	6.562	6.119	3.062	2.255

[1] the two values of distances correspond to the two Me_2btp ligands

References

1   W. G. Finnegan, R. A. Henry and R. Lofquist, *J. Am. Chem. Soc.*, 1958, **80**, 3908–3911.

2   J. M. McManus and R. M. Herbst, *J. Org. Chem.*, 1959, **24**, 1462–1464.

3   M. Attolini, T. Boxus, S. Biltresse and J. Marchand-Brynaert, *Tetrahedron Lett.*, 2002, **43**, 1187–1188.

4   G. M. Sheldrick, SADABS-2008/1 - Bruker AXS Area Detector Scaling and Absorption Correction, Bruker AXS, Madison, WI 2008.

5   G. M. Sheldrick, *Acta Crystallogr. Sect. C*, 2015, **71**, 3–8.

6   C. F. Macrae, I. Sovago, S. J. Cottrell, P. T. A. Galek, P. McCabe, E. Pidcock, M. Platings, G. P. Shields, J. S. Stevens, M. Towler and P. A. Wood, *J. Appl. Crystallogr.*, 2020, **53**, 226–235.

7   G. A. Bain and J. F. Berry, *J. Chem. Educ.*, 2008, **85**, 532–536.

8   M. J. Frisch, G. W. Trucks, H. B. Schlegel, G. E. Scuseria, M. A. Robb, J. R. Cheeseman, G. Scalmani, V. Barone, B. Mennucci, G. A. Petersson and et al., Gaussian 16 , Revision B.01 Gaussian, Inc., Wallingford, CT, USA 2016.

9   Y. Zhao and D. G. Truhlar, *Theor. Chem. Acc.*, 2008, **120**, 215–241.

10 M. C. D. Llunell, P. A. J. Cirera and S. Alvarez, Shape program, 2nd ed; Universitat de Barcelona: Barcelona, Spain (version Second Edition) 2010.